The role of specific PP2A complexes in the dephosphorylation of γ-H2AX

Liping Chen[1,*], Yandong Lai[1,5,*], Xiaonian Zhu[1,*], Lu Ma[1], Qing Bai[1], IriaVazquez[2], Yongmei Xiao[1], Caixia Liu[1], Daochuan Li[1], Chen Gao[1], Zhini He[1], Xiaowen Zeng[1], Xiumei Xing[1], Zhengbao Zhang[1], Jie Li[1], Bo Zhang[1], Qing Wang[1], Anna A. Sablina[2], William C. Hahn[3,4], and Wen Chen[1,#]

[1]*Department of Toxicology, School of Public Health, Sun Yat-sen University, Guangzhou 510080, China;*

[2]*VIB Center for the Biology of Disease; KU Leuven Center for Human Genetics, B-3000 Leuven, Belgium;*

[3]*Department of Medical Oncology, Dana-Farber Cancer Institute, Boston, MA 02115, USA*

[4]*Broad Institute of MIT and Harvard, Cambridge, MA 02142, USA*

[5]*Institute for Chemical Carcinogenesis, Guangzhou Medical University, Guangzhou 510182, China*

[*]These authors contributed equally to this work.

[#]To whom correspondence should be addressed. Tel: +011 86 20 87330599; Fax: +011 86 20 87330446; E-mail: chenwen@mail.sysu.edu.cn.

Running title: PP2A B56ε complexes dephosphorylate γ-H2AX

JCS Advance Online Article. Posted on 18 September 2014

Word count: 7673 (minus refs)

Number of figures: 6

Supplemental figures: 4

Summary

The formation of γ-H2AX in response to DNA double-strand breaks (DSBs) marks damaged regions for recognition and repair. Dephosphorylation of γ-H2AX is required for cells to resume cell cycle. However, the mechanisms of γ-H2AX dephosphorylation remain underexplored. Using a loss of function screen, we identified PP2A specific subunits, B56ε and α4, involved in elimination of γ-H2AX during DSBs repair process. In the early stage of DSBs repair the inhibitory subunit α4 binds and renders PP2Ac inactive. As DNA is repaired, α4 releases PP2Ac and triggers the assembly of an active PP2A B56ε holoenzyme. PP2A B56ε, which translocates from cytoplasm into the nucleus upon DNA damage, is responsible for a direct dephosphorylation of γ-H2AX. Suppression of both B56ε and α4 leads to persistence of γ-H2AX and defects in DNA repair. In contrast, the rapid clearance of γ-H2AX in human hepatocarcinoma is correlated with the over-expression of both B56ε and α4. Functional analysis reveals that PP2A B56ε coordinates with α4 in accelerating HR repair upon DNA damage. Together, these observations gain insight of how γ-H2AX dephosphorylation is kinetically regulated during DNA repair response.

Keywords: γ-H2AX; α4; PP2A B56ε subunit; human cells; DNA repair

Introduction

Mammalian cells exposed to DNA damaging agents trigger important defensive pathways by inducing multiple proteins involved in DNA repair, cell cycle checkpoint control, protein translocation and degradation. DNA damage induces structural alterations to DNA, which can be detected by DNA repair mechanisms (Jackson, 2002). Once damage is identified, specific DNA repair molecules are recruited at or near the sites of damage, inducing other molecules to bind and form a complex that enables DNA repair (Rogakou et al., 1999). The failure to repair DNA facilitates genomic instability, which in turn may result in cell death or increase the risk of pathological consequences such as cancer development.

In eukaryotic cells, the induction of DNA double-strand breaks (DSBs) in chromatin promptly initiates the phosphorylation of the histone H2A variant, H2AX, at Serine 139 to generate γ-H2AX (Rogakou et al., 1998). The phosphorylation of H2AX is critical in maintaining the genome stability (Shrivastav et al., 2008). H2AX-deficient mice display higher radiosensitivity, chromosome instability, and enhanced cancer susceptibility. In addition, these mice exhibit repair defects and impaired recruitment of DNA repair proteins including NBS1, 53BP1, and BRCA1 to irradiation-induced foci (Celeste et al., 2003; Celeste et al., 2002). These observations establish a key role for γ-H2AX in the activation of DNA damage response (DDR).

The phosphorylation of H2AX is one of the early events in response to DNA DSBs (Fernandez-Capetillo et al., 2004; Rogakou et al., 1998; Tomita, 2010). γ-H2AX serves as a signal to promote the recruitment of DNA repair proteins to the site of DSB, activate cell cycle checkpoints, and prevent unrepaired DNA to pass into daughter cell during replication (Kinner et al., 2008). Together with distinct histone modifications, γ-H2AX foci anchor additional DDR proteins near DSBs to complete DSBs repair (Fillingham et al., 2006; Huertas, 2010; Xu and Price, 2011). The assembly of proteins at the DSB-flanking chromatin occurs in a highly ordered

fashion, which can be achieved by regulation of protein-protein interactions triggered by a variety of posttranslational modifications (PTMs) (Kinner et al., 2008). Accordingly, the disrupted histones must be re-deposited onto DNA to restore the chromatin structure following the completion of DNA repair (Xu and Price, 2011). Although the Ser/Thr protein kinases that are responsible for γ-H2AX formation have been well studied, how γ-H2AX is eliminated in mammalian cells after DSBs rejoining and the functional consequences of persistence of phosphorylated H2AX are not clearly elucidated. However, it is clear that the removal of γ-H2AX from sites of DNA damage is tightly regulated to restore chromatin integrity of mammalian genomes upon completion of DNA repair to block the dissociation of repair proteins and release from cell cycle checkpoint (Keogh et al., 2006). H2AX phosphorylation signal is putatively removed by the joint action of histone exchange and phosphatases (Keogh et al., 2006; Kusch et al., 2004). Indeed, several lines of evidence indicate that dephosphorylating γ-H2AX is regulated by multiple phosphatases in mammalian cells, including protein phosphatase 2A (PP2A) (Chowdhury et al., 2005), PP4 (Chowdhury et al., 2008; Nakada et al., 2008), PP6 (Douglas et al., 2010) and Wip1 (Cha et al., 2010). However, the comprehensive mechanistic understanding how phosphatases regulate γ-H2AX is far from complete. In this study, we focus on the dynamic regulation of PP2A on γ-H2AX dephosphorylation.

Protein phosphatase 2A (PP2A) is a large family of holoenzymes that accounts for the majority of Ser/Thr phosphatase activity in eukaryotic cells (Shi, 2009). PP2A enzymes are ubiquitously expressed proteins that are implicated in diverse cell processes (Janssens and Goris, 2001). Most PP2A exists in two general forms, a heterodimeric complex of scaffolding A subunit (PR65) and a catalytic C subunit (PP2Ac subunit) and a heterotrimeric enzyme that also includes B subunits. The association of the core enzyme with a variety of regulatory B-type subunit generates many distinct holoenzymes. Four distinct B-type protein families, named as B (B55 and PR55), B′ (B56 and PR61), B″ (PR72, PR130, PR59 or PR48) and B‴ (PR93/SG2NA or PR110/Striatin), have been identified. The functional diversity,

substrate specificity and sub-cellular localization of this enzyme are conferred by their distinct B-type regulatory subunit (Xu et al., 2006; Zhao et al., 1997). In addition to binding to PR65/A subunit, a small proportion of PP2Ac associates with Tap42/α4, an interaction mutually exclusive with that of PR65/A (Di Como and Arndt, 1996; Prickett and Brautigan, 2004). This interaction leads to inactivation of PP2A enzyme activity and shelters PP2Ac from degradation (Kong et al., 2009). Although it has been found that PP2A directly dephosphorylates γ-H2AX (Chowdhury et al., 2005), which specific PP2A regulatory B subunit is involved and how PP2A is regulated during the DNA DSB repair remains undefined. Here we show that γ-H2AX is a direct substrate of holoenzymes PP2A B56ε, whereas α4 plays a key role in regulating PP2A activity and formation of B56ε heretrimeric holoenzymes during DNA DSBs repair.

Results

Suppression of specific PP2A regulatory subunits led to persistence of γ-H2AX

A prior study revealed that PP2A catalytic subunit C (PP2Ac) interacts and dephosphorylates γ-H2AX (Chowdhury et al., 2005). In consonance with this observation, suppression of the PP2A scaffolding subunit Aα results in persistent γ-H2AX expression upon camptothecin (CPT) administration. To identify specific PP2A holoenzymes involved in γ-H2AX dephosphorylation, we performed a loss-of-function screen in immortal human embryonic kidney cells (HEK cells) expressing SV40 LT and the telomerase catalytic subunit (*hTERT*). We generated a series of stable HEK cell lines by infecting cells with lentivirally delivered short hairpin RNAs (shRNAs) specific for each of PP2A B regulatory subunits. HEK SHGFP cells expressing a shRNA targeting GFP (shGFP) were used as a control. To eliminate the contribution of off-target effects, we selected two independent shRNAs that targeted different sequences in each of PP2A regulatory subunit. The suppression of PP2A subunits by shRNAs was confirmed by immunoblotting analysis (Fig. 1A and Fig. S1A). Importantly, suppression of individual PP2A B subunits such as B55α, B56γ, or B56ε, did not affect the stability of other PP2A subunits (Fig. S2A), indicating that the generated cell lines allow us to assess the effects of knockdown of individual PP2A subunit.

We next assessed how suppression of individual PP2A B regulatory subunit affects regulation of γ-H2AX by analyzing γ-H2AX levels in HEK cells expressing PP2A shRNAs after CPT treatment. The amount of γ-H2AX in HEK cells expressing shGFP attenuated rapidly and was almost at the basal level at 16 h after CPT treatment. On the other hand, γ-H2AX was not cleared even after 16 h in HEK cells expressing shB55α, shB56ε, or shα4 (Fig. 1B). The similar results were observed in HepG2 cells after suppression of PP2A B55α, B56γ, B56ε, or α4 cells (Fig. S3A). We also revealed sustained γ-H2AX expression in HEK SHB55α, SHB56ε, and SHα4 cells after treatment with another DNA damaging agent,

N-methyl-N′-nitro-N-nitrosoguanidine (MNNG) (Fig. S1B). In contrast, suppression of PP2A B56γ led to a decreased amount of γ-H2AX (Fig. 1A). Therefore, we found that in addition to PP2A Aα, suppression of B55α, B56ε, or α4 subunit resulted in persistence of γ-H2AX compared to cells expressing shGFP (Fig. 1A).

To confirm the results of immunoblotting analysis, we examined the number of γ-H2AX foci in HEK cells expressing PP2A shB55α, shB56γ, shB56ε, or shα4 at different time points following CPT treatment by immunofluorescence assay. We found that depletion of B56γ significantly decreased the number of γ-H2AX foci and attenuated foci intensity (P<0.01) at both 2 h and 12 h after CPT treatment. As shown in Fig.1C, suppression of B55α resulted in a significant increase in number of γ-H2AX foci (P<0.05) at both 2 h and 12 h after CPT treatment compared with SHGFP cells, consistent with our previous observations showing that B55α is directly involved in regulation of ATM phosphorylation (Kalev et al., 2012b).

The different kinetics was observed in HEK cell lines expressing shB56ε or shα4. Although the number of γ-H2AX foci in HEK cell lines expressing shGFP, shB56ε, or shα4 was similar at 2 h after CPT removal, the foci clearance was dramatically delayed in cells with suppressed expression of B56ε or α4 (Fig. 1C). Taken together, these observations indicate that level of γ-H2AX after DNA DSBs is regulated by specific PP2A holoenzymes. Moreover, the kinetics of γ-H2AX foci suggests that PP2A B56ε or α4 may regulate the clearance of γ-H2AX foci.

PP2A B56ε holoenzyme is responsible for γ-H2AX dephosphorylation

The prolonged kinetics of γ-H2AX in cells with suppressed expression of B56ε or α4 suggests that PP2A B56ε or α4 regulatory subunits may contribute to γ-H2AX dephosphorylation. To test this idea, we transiently expressed HA-tagged B55α, B56γ, B56ε, and α4 in 293FT cells and performed co-immunoprecipitation (co-IP) assays using HA-specific antibody. Consistently to our hypothesis, we found that both PP2A

B56ε and α4 were in complex with γ-H2AX and PP2A catalytic subunit Cα (PP2Ac) (Fig. 2A). We also detected these interactions between endogenous proteins in CPT-treated cells by isolating the nuclear fractions and performing a set of reciprocal co-IPs (Fig. 2B). Strikingly, the substitution of Ser139 of H2AX to alanine (Mut-H2AX) completely abolished the interaction with Aα, B56ε, PP2Ac, or α4, indicating that PP2A complexes specifically interact with γ-H2AX, but not with non-phosphorylated H2AX (Fig. 2C).

Previous studies have demonstrated that PP2A B56ε localized mostly in the cytoplasm (McCright et al., 1996; Strack et al., 1998). Therefore, we determined how DNA damage affects cellular localization of PP2A B56ε. Immunofluorescent analysis of HA-tagged B56ε revealed that in HEK SHGFP cells treated with vehicle DMSO B56ε was primarily localized in the cytoplasm, whereas CPT treatment triggered its translocation from the cytoplasm to the nucleus. In contrast, we did not observe any re-localization of B55α or B56γ (Fig. 2D) in cells treated with CPT. We also examined the presence of PP2A B56ε in nuclear and cytoplasmic fractions isolated from CPT-treated HEK cells. As shown in Fig. 2E, the amount of B56ε in the nuclear fraction increased 2-fold at 1 h and remained at high level at 5 h and 10 h after CPT treatment. Correspondingly, the level of PP2A B56ε in cytoplasmic fraction decreased at 5 h after addition of CPT. In contrast, the sub-cellular localization of PP2A B55α, B56γ, and α4 remained unchanged (Fig. 2D, E).

We next analyzed co-localization between B56ε and γ-H2AX during DNA repair response by counting the total number of γ-H2AX foci and the number of the foci where γ-H2AX and B56ε co-localized. We found that the number of merging dots was 4.3±2.2% 1 h after CPT treatment removal, while 5 h upon DNA damage it increased up to 54.0±10.1%. In contrast, we failed to detect co-localization of B55α or B56γ with γ-H2AX. Taken together, these observations indicate that γ-H2AX might be a direct target of holoenzyme PP2A B56ε.

198 **α4 is essential for recruitment of PP2A B56ε by γ-H2AX**

199 The findings that γ-H2AX clearance is sustained in α4-depleted cells and α4
200 forms a complex with γ-H2AX suggest that α4 may regulate PP2A-attributable
201 γ-H2AX dephosphorylation. To test this hypothesis, we assessed the order by which
202 different components of PP2A complexes are recruited to γ-H2AX in the course of
203 DSB repair response as well as PP2A-attributable phosphatase activity at different
204 time points after DNA damage.

205 We found that 1 h after CPT treatment PP2Ac interacted with α4, but not with
206 γ-H2AX, suggesting that binding α4 to PP2Ac took place before recruitment to
207 γ-H2AX foci. 5 h upon CPT treatment, both α4 and PP2Ac formed a complex with
208 γ-H2AX (Fig. 3A), indicating that α4/PP2Ac complex is recruited to γ-H2AX foci in
209 the course of DNA repair. Importantly, we found that α4 bound PP2Ac and γ-H2AX
210 in the absence of A- and B-subunits (Fig. 2B) that is in consonance with a previous
211 study (Nanahoshi et al., 1999). Moreover, 10 h upon CPT treatment α4 is dissociated
212 from γ-H2AX.

213 PP2A regulatory B56ε subunit demonstrated a different kinetics of interaction
214 with γ-H2AX. In contrast to α4, PP2A B56ε formed a complex with γ-H2AX mainly
215 at 5 h after CPT removal (Fig. 3A), indicating that the assembly of PP2A B56ε
216 holoenzyme at γ-H2AX foci occurs at late stages of DSB repair (Fig. 3A). The later
217 observation also suggests α4 may play an essential role in regulating the assembly of
218 PP2A complexes, as it has been previously described (Prickett and Brautigan, 2004).

219 To test this idea, we examined how α4 affected the formation of PP2A B56ε
220 holoenzymes and their recruitment by γ-H2AX. We found that suppression of α4 did
221 not affect B56ε translocation from cytoplasm to nucleus upon DNA damage (Fig.
222 3C). However, we found that α4 depletion significantly impaired the interaction
223 between γ-H2AX and both PP2A Aα and B56ε subunits (Fig. 3D). These
224 observations indicate that the defects of α4 abolish the recruitment of PP2A B56ε
225 holoenzyme to γ-H2AX foci, suggesting that dissociation of α4 from

γ-H2AX/PP2Ac complexes may facilitate the assembly of PP2A B56ε-specific heterotrimeric holoenzymes.

In parallel, we detected PP2A-attributable phosphatase activity using mononucleosomes containing γ-H2AX as a substrate (Fig. 3B, top left lane) in 293FT cells at different time points after CPT removal. We found that PP2A activity was reduced by 36.4±4.7% at 1 h, but increased by 102.3±7.9% at 5 h compared to control cells. Finally, 10 h after DNA damage PP2A activity was similar to what was observed in untreated cells (Fig. 3B). Decreased PP2A phosphatase activity in the nucleus at early stages of DNA repair could be explained by the increased interaction between α4 and PP2Ac at 1 h upon DNA damage, as α4 is known to inhibit PP2A activity (Kong et al., 2009). On the other hand, increased PP2A activity 5 h after CPT removal correlates to the assembly of catalytically active PP2A B56ε holoenzymes (Fig. 3A). Notably, the formation of active PP2A B56ε complexes and enhanced PP2A activity (Fig. 3A) are correlated with the rapid decline of γ-H2AX (Fig. 1B). Taken together, these results strongly implicate both α4 and B56ε in regulation of γ-H2AX dephosphorylation.

PP2A B56ε and α4 are involved in DSB repair

The roles of α4 and B56ε in dephosphorylation of γ-H2AX suggest their contributions in regulating DNA repair response. To address this issue, we measured the persistence of DSB in CPT-treated HEK cells expressing shRNAs specifically targeting B56ε or α4 using the neutral single-cell gel electrophoresis assay (Comet assay). As a result, 12 h after CPT treatment removal, the Tail Moment values were significantly higher in HEK cells expressing either shB56ε or shα4 than in control cells. In contrast, the Tail Moment value in HEK SHB56γ was significantly lower than in control cells ($P<0.01$) (Fig. 4A).

In addition to Comet assay, we performed cytokinesis-block micronucleus assay

(CBMN) to examine the degree of DNA damage and genome instability by measuring the frequencies of micronuclei formation upon DNA damage. The formation of micronuclei is the result of chromosome breakage and loss due to un-repaired or mis-repaired DNA lesions or chromosome malsegregation due to mitotic malfunction (Fenech, 2002). We found that the frequencies of micronuclei in 1000 binucleated cells in response to mitomycin C (MMC) treatment increased by 40.1±6.4% or 52.0±3.9%, respectively in HEK SH56ε (P<0.01) or HEK SHα4 (P<0.05) cells compared to control cells (Fig. 4B), indicating that suppression of B56ε or α4 confers hypersensitivity to DNA damage and increased genome instability.

We next examine how B56ε or α4 affects two major pathways for DSBs repair, homologous recombination (HR) and non homologous end joining (NHEJ) (Sonoda et al., 2006). To this end, we tested HR-mediated I-SceI-induced DSB repair in 293 DR-GFP cells and NHEJ-mediated repair of a linearized GFP reporter construct. We found that suppression of B56ε decreased the efficiency of HR repair, but had little effect on NHEJ repair. In parallel, suppression of α4 inhibits both HR and NHEJ DNA repair, suggesting that α4 may contribute to DNA repair by regulating formation of several PP2A complexes in addition to B56ε specific complexes. In contrast, the deficiency of B56γ had no obvious effect on both HR and NHEJ repair pathways (Fig. 4C, D). These results indicate that loss of B56ε or α4 impair DNA repair by affecting HR and/or NHEJ repair pathways.

Inhibition of DNA repair observed in B56ε- or α4-depleted cells also suggests that these cells are highly sensitive to DNA damage. Indeed, we found that suppression of PP2A B56ε or α4 resulted in decreased cell viability in response to CPT, MNNG, or MMC treatment (Fig. S2B). Similar results were found when we analyzed cell viability of a human hepatoma HepG2 cells expressing shRNAs targeting PP2A B56ε or α4 (Fig. S3B). Together, these observations indicate that dysregulation of γ-H2AX dephosphorylation due to loss of particular PP2A regulatory subunits impair DNA repair.

PP2A B56ε cooperates with α4 to control HR DNA repair

To further address the role of B56ε and α4 on DNA repair, we generated HEK cells stably expressing α4, B56ε, or both α4 and B56ε. We confirmed overexpression of α4 and B56ε by immunoblotting analysis (Fig. 5A). In addition, we found that the up-regulation of B56ε or α4 displayed no change on γ-H2AX clearance after CPT treatments. However, immunoblotting analysis revealed that the γ-H2AX clearance in HEK-B56ε-α4 cells was greatly improved compared to that in HEK-vector cells (Fig. 5B), indicating that B56ε and α4 may cooperate in rapid dephosphorylation of γ-H2AX upon DNA damage. Consistent with these findings, we found that the Tail Moment values were significantly lower in HEK-B56ε-α4 cells than HEK-vector cells at 12 h after CPT treatment removal ($P<0.05$) (Fig. 5C), implying that B56ε and α4 work together in promoting the DNA repair.

To further clarify the role of B56ε and α4 in modulating DSB repair, we examined the effects of B56ε and α4 over-expressions on two major pathways of DSB repair, NHEJ and HR. We found that simultaneous overexpression of both B56ε and α4 led to a 71.7±8.3% increase in HR repair, but had no impact on the NHEJ repair. In addition, over-expression of individual PP2A subunit had no obvious effects on either HR, or NHEJ repairs (Fig. 5D, E). Together, these results support the notion that B56ε and α4 cooperate to facilitate HR DNA repair pathway.

Expression of PP2A B56ε and α4 in carcinogen-transformed cells and human cancers

The contribution of B56ε and α4 in γ-H2AX dephosphorylation suggests the role of these PP2A subunits in cancer development and progression. Therefore, we determined how B56ε or α4 affected DNA repair response in carcinogen-transformed cells. Consistent with our previous findings that α4 is highly

expressed in carcinogen-transformed human cells and primary human cancers (Chen et al., 2011), we found that the expressions of α4 in L02RT-AFB_1 cells were significantly increased compared to L02 cells (Fig. 6A). Notably, we found that PP2A B56ε was over-expressed in transformed cells L02RT-AFB_1 (Fig. 6A). Immunoblotting analysis of γ-H2AX after treatment of hepatic cells with CPT revealed that γ-H2AX clearance in L02RT-AFB_1 cells was much faster than that in L02 cells (Fig. 6B). We speculate that high levels of B56ε and α4 may be associated with rapid dephosphorylation of γ-H2AX upon DNA damage. To further define the role of B56ε and α4 in regulation of γ-H2AX, we introduced shRNAs that target B56ε or α4 into L02 and L02RT-AFB_1 cells. We showed that the suppression of B56ε or α4 led to a substantial accumulation of γ-H2AX after CPT treatment. In particular, the difference in γ-H2AX levels between untreated- and CPT treated-L02RT-AFB_1 cells were more pronounced compared to L02 cells (Fig. S4), suggesting that up-regulation of B56ε and α4 may facilitate the rapid γ-H2AX dephosphorylation. More importantly, we showed that 12 h after CPT treatment removal, the Tail Moment values were significantly lower in L02RT-AFB_1 cells than in L02 cells ($P<0.05$) (Fig. 6C).

Moreover, when we determined the expression of B56ε and α4 in 14 paired human primary hepatocellular carcinoma (HCC) and matched adjacent non-tumor tissues, we found overexpression of α4 (13/14) and B56ε (10/14) appearing in HCC specimens. In contrast, the γ-H2AX expression in HCC tissues was down-regulated comparing to the matched adjacent non-tumor tissues (Fig. 6D). We speculate that the over-expression of the PP2A subunits may play a role in the rapid clearance of γ-H2AX in malignant carcinoma cells. Taken together, these findings indicate that up-regulation of B56ε and α4 may facilitate fast repair of DNA damage lesions in tumor cells.

Since dephosphorylation of γ-H2AX is one of rate-limiting factors involved in recovery from DNA damage induced cell cycle arrest (Bartek and Lukas, 2007), we examined whether cell cycle was affected in cells expressing α4, or B56ε, or both α4

and B56ε. CPT is a topoisomerase inhibitor and forms topoisomerase I cleavage complexes, which are converted into DNA DSB through DNA replication (Strumberg et al., 2000). Thus, it activates a replication checkpoint in the S-phase (Shao et al., 1999). Consistent with previous studies, we observed that S-phase arrest in HEK-vector cells at 8 h after CPT removal, while no obvious changes in CPT-triggered S-phase arrest in HEK-α4 or HEK-B56ε cells. However, ectopic expression of both B56ε and α4 significantly facilitated S-G_2 phase transition (Fig. 6E), suggesting that high levels of both B56ε and α4 are required for accelerating the release from S phase arrest during DSBs repair. Taken together, these findings demonstrate that the B56ε and α4 function collaboratively in promotion of the DSB repair and confer cells with a fast cell growth state.

Discussion

Reversible phosphorylation plays critical roles in numerous cellular events, including the response to DNA double-strand breaks (DSBs). The formation of γ-H2AX triggers recruitment of DNA repair proteins to the sites of DSBs (Fernandez-Capetillo et al., 2002; Kolas et al., 2007; Melander et al., 2008; Stucki et al., 2005; Stucki and Jackson, 2006), whereas the elimination of γ-H2AX is required for dissociation of repair proteins and recovery from cell cycle checkpoint arrest (Keogh et al., 2006). Although several types of phosphatases have been shown to be directly involved in γ-H2AX dephosphorylation (Chowdhury et al., 2005; Chowdhury et al., 2008; Douglas et al., 2010; Keogh et al., 2006), our data strongly indicate that γ-H2AX was found predominantly in complexes with PP2Ac (data not shown), highlighting the importance of PP2A in control of γ-H2AX clearance. Here we investigate the roles for specific PP2A regulatory subunits in dynamic regulation of γ-H2AX removal.

We found that suppression of PP2A B subunits, B55α and B56ε, and the PP2A regulating protein α4 leads to the persistence of γ-H2AX, implicating that these specific PP2A subunits in regulation of DNA DSB repair. In our previous study, we revealed that B55α subunit is responsible for increased phosphorylated ATM and the activation of kinase CHK2 that leads to cell cycle arrest and the suppression of BRCA1 and RAD51 (Kalev et al., 2012a). On the other hand, in this report, our results strongly indicate that B56ε and α4 function in a tightly controlled manner during DSBs repair to regulate timely dephosphorylation of γ-H2AX. This confirms that distinct PP2A heterotrimeric complexes contribute to DDR by targeting multiple substrates in a spatially- and temporally-specific manner. In addition, PP2A B56γ previously has been shown to be crucial for activating p53 during DNA damage response (Shouse et al., 2011). Consistently, here we revealed that PP2A B56γ subunit suppression led to a rapid γ-H2AX dephosphorylation. However, there is no evidence supporting an idea that B56γ directly regulates the process of γ-H2AX dephosphorylation. It is possible that PP2A B56γ depletion perturbs the composition

of other PP2A B56 subunits (Chen et al., 2004), leading to the alteration of the assembly of PP2A complexes and the rate of γ-H2AX clearance.

Our results suggest that PP2A B56ε-containing holoenzymes directly dephosphorylate γ-H2AX, whereas PP2A B56ε-deficient cells exhibited impaired HR DNA repair and hypersensitivity to DNA damaging agents. Consistently with our results, a previous study also demonstrated that PP2A B56ε protects cells from CPT-induced apoptosis (Jin et al., 2010). Moreover, a recent report identified a link between B56ε and human soft tissue sarcoma. It was revealed that ε-SNP2, a SNP located in the third intron of B56ε, associates with increased risk of human soft tissue sarcoma. Although it remains unclear how ε-SNP2 affects activity of PP2A B56ε complexes, it raises the possibility that B56ε plays an important role in DNA repair response (Grochola et al., 2009). Suppression of the cellular regulator α4 also impairs DSBs repair (Sents et al., 2013). Prior work demonstrated that α4 plays an essential role in regulating the assembly and maintenance of PP2A complexes by stabilizing the free PP2Ac (Kong et al., 2009; Kong et al., 2004). Recent study also showed that α4 promotes assembly of an adaptive PP2A complex containing B55α subunit upon glutamine deprivation (Reid et al., 2013). The structure of Tap42/α4 reveals that the highly conserved domain of Tap42 (the yeast α4-homologue) possesses an all-α-helical structure and functions as adaptors and scaffolds, which suggests mechanisms by which PP2Ac substrate specificity and ubiquitination is regulated (McConnell et al., 2010; Smetana et al., 2006; Trockenbacher et al., 2001; Yang et al., 2007).

Our prior work identified that α4 contributes to carcinogen-induced transformation. The reduction of PP2A activity due to enhanced α4-PP2Ac interaction contributes directly to chemical carcinogen-induced tumorigenesis (Chen et al., 2011). The catalytic subunits of the protein serine/threonine phosphatase 2A-like family (PP4 and PP6) also form complexes with α4 (Kloeker et al., 2003) and the depletion of α4 leads to progressive loss of all PP2A, PP4, and PP6 phosphatase complexes (Kong et al., 2009), suggesting that the role of α4 in regulation of numerous biological

processes. Here we demonstrate that the interaction between α4 and PP2Ac not only prevent PP2Ac from degradation but also facilitate assembly of PP2A B56ε heterotrimeric complexes associated with γ-H2AX.

γ-H2AX is commonly used as a biomarker of cellular response to DSBs and in monitoring DNA damage and repair(Valdiglesias et al., 2013) and as a pharmacodynamic marker for monitoring effects of radionuclide therapy in clinical studies (Guzi et al., 2011; Rothkamm and Lobrich, 2003). We found low level of γ-H2AX in chemical carcinogen-transformed human cells and human primary hepatocellular carcinomas. Importantly, low levels of γ-H2AX in these cells are associated with high expression of B56ε and α4, suggesting that rapid dephosphorylation of γ-H2AX in both B56ε-α4 over-expressed cells promotes DNA repair and allows cells to escape from chemical-induced cell cycle checkpoint arrest. In fact, transformed malignant cells exhibit high levels of γ-H2AX caused by endogenous DSBs due to dysfunctional telomeric DNA damage, hypoxia, reactive oxygen species (ROS), or replication stress (Harding et al., 2011; Murnane, 2010; Nabb et al., 2006). The maintenance of the key factors of DNA repair is crucial in promoting cell survival of tumors cells (Abbotts et al., 2014). With respect to γ-H2AX, we speculate that the temporal- and spacial-regulation of γ-H2AX dephosphorylation are crucial to control the rate of DSBs repair. The dysregulation of PP2A activity or complex composition that leads to a rapid γ-H2AX dephosphorylation may facilitate survival of tumor cells.

In summary, we found that PP2A B56ε is responsible for dephosphorylation of γ-H2AX during DSB repair. PP2Ac is recruited to γ-H2AX in complex with α4, and the subsequent release of PP2Ac from α4 leads to the assembly of activated PP2A B56ε holoenzymes. Loss of either PP2A B56ε or α4 leads to defects in DNA repair that promotes genomic instability. These findings provide new insights into the mechanisms that regulate the repair of DNA damage and elucidate the roles of specific phosphatase complexes in DNA damage responses.

MATERIAL AND METHODS

Reagents and Antibodies

Mitomycin C (MMC) and complete protease inhibitor cocktail tablets were purchased from Roche. Hydroxyurea (HU), Camptothecin (CPT), N-methyl-N'-nitro-N-nitrosoguanidine (MNNG), and cytochalasin B (cyt-B) were obtained from Sigma-Aldrich (St. Louis, MO, USA). The following antibodies were used: mouse anti-γ-H2AX (clone JBW301), rabbit anti-H2AX and mouse anti-PP2A Cα (clone 1D6) (Upstate Biotechnology, NY), rabbit or mouse anti-HA tag (Cell Signaling Technology, Danvers, MA, USA), rabbit anti-PPP4C and -PPP6C (Bethyl Laboratories, Montgomery, TX, USA), rabbit polyclonal anti-α4, B56α, and B56β (Novus, Littleton, CO), rabbit anti-B55γ, PR130 PR110, and PTPA (Proteintech Group, Chicago, IL, USA), and rabbit anti-B55δ and PR93 (Gene Tex, Irvine, CA, USA). The B55α, B56ε, B56γ and B56δ polyclonal antibody were prepared as previously described (Chen et al., 2005).

Cell lines and establishment of stable cell lines

Human embryonic kidney cells expressing Simian Virus 40 LT antigen (LT) and the telomerase catalytic subunit (*hTERT*) (HEK cells) were generated as described previously (Hahn et al., 1999).

The pLKO.1-puro shGFP and pLKO.1-puro vectors containing short hairpin RNA (shRNA) targeting specific PP2A subunits (Table S1) were provided by the RNAi Consortium (Moffat et al., 2006). To create a HA-tagged version of PP2Asubunits, we performed PCR with specific primers (Table S2) to generate retroviral vectors, pBabe-HA-B55α, pBabe-HA-B56γ, pBabe-HA-B56ε, and pBabe-HA-α4.

Cell proliferation assays

To measure cell proliferation , 2×10^4 cells were plated in triplicate and harvested at the indicated time. The number of cells was determined by a Z2 Particle Count and Size Analyzer (Beckman-Coulter, Miami, FL). Cell viability was measured by MTT assay, 8×10^3 cells per well were seeded on a 96-well plate in quadruplicates for 24 h, and treated with various concentrations of DNA damage agents, then cultured for an additional 24 h. Cell Proliferation kit (WST-1) was used for the assay according to the manufacturer's protocol.

Separation of cytoplasmic and nuclear fractions

Cells were resuspended in a hypotonic buffer [20 mM Tris-HCl (pH 7.2), 15 mM KCl, 2.5 mM MgCl2, 0.05% NP-40 and mixed protease inhibitors] on ice for 10 min, and suctioned with a needle. The homogenate was then centrifuged at 3,000×g for 5 min at 4°C. The supernatants were collected and the nuclear pellets were resuspended in extraction buffer [50 mM Tris-HCl (pH 7.8), 150 mM KCl, 5 mM $MgCl_2$, 250 mM sucrose and mixed protease inhibitors], followed by a micrococcal nuclease (MNase) (Takara) digestion for 15 min at 37°C. The nuclear extracts were placed on top of a cushion containing 0.88 M sucrose in the extraction buffer. The mixture was centrifuged at 16,000×g for 15 min and soluble nuclear fraction was collected.

Immunoblotting and co-immunoprecipitation

The frozen tissue samples were pulverized by mortar and pestle in liquid nitrogen, and reconstituted in ice-cold RIPA lysis buffer [150 mM NaCl, 1% Triton X-100, 0.5% deoxycholate, 0.1% SDS, and 50 mM Tris (pH7.4)] containing protease inhibitors for 30 min. The lysates were centrifuged at 12,000×g

for 20 minutes at 4°C.

For analysis of γ-H2AX levels, cells were lysed directly on the plate using 2×SDS sample buffer [125 mM Tris-base, 138 mM SDS, 10% β-mercaptoethanol, 20% glycerol, bromophenol blue (pH 6.8)]. For immunoprecipitation analysis, 2-3 mg nuclear fractions were incubated with specific antibodies at 4°C overnight. 100 µl of prewashed 1:1 slurry of protein G sepharose was added to the mixture and incubated for additional 2 h. The protein G beads/protein complexes were washed three times and eluted in 2×SDS loading buffer, followed by SDS-PAGE and immunoblotting.

Mononucleosome preparation

Mononucleosomes containing human γ-H2AX were prepared as described (Barsoum and Varshavsky, 1985). Briefly, 293FT cells were treated with 2 µM CPT for 1 h. The cell pellets were resuspended and washed twice in ice-cold buffer A (20 mM HEPES, 10 mM KCl, 1.5 mM $MgCl_2$, 0.34 M sucrose, 10% glycerol, 1 mM DTT, 1 mM PMSF, and 10 mM NEMI), and centrifuged at 600×g for 5 min. The nuclear pellet was resuspended in buffer B (20 mM HEPES, 10 mM KCl, 1.5 mM $MgCl_2$, 0.34 M sucrose, 10% glycerol, 1 mM DTT, and 2 mM $CaCl_2$) followed by the addition of micrococcal nuclease and digestion at 37°C for 30 min. The digestion was stopped by 1 mM EGTA and centrifuged at 600×g for 5 min. The precipitate was resuspend in nuclear extraction buffer (20 mM HEPES, 420 mM NaCl, 1.5 mM $MgCl_2$, and 0.2mM EGTA) for 1 h on ice, then centrifuged at 1000×g for 5 min. After that, the dilution and equilibration buffer (20 mM HEPES, 1.5mM $MgCl_2$, 0.2 mM EGTA, and 25% glycerol) was added to the supernatant followed by centrifugation. The supernatant was collected as mononucleosomes and storage at -80°C.

Detection of PP2A-attributable protein phosphatase activity

PP2A activity was measured using a Ser/Thr Phosphatase Assay Kit (Millipore, Billerica, MA) with modification. Briefly, 500 μg of nuclear fraction were incubated with antibody against PP2Ac at 4°C overnight. Then 35 μl 50% protein G sepharose beads were added and incubated at 4°C for additional 2 h. The beads were washed with phosphate buffer solution before incubation with mononucleosome substrates. The samples were centrifuged briefly, and 25 μl samples were transferred into a well of a 96-well microtiter plate. A detection solution containing malachite green (100 μl) was added and incubated for 15 min at RT. A colorimetric assay was made by reading at 630 nm in a microtiter plate reader. Absorbance values of samples were compared with negative controls containing no enzyme and a freshly prepared phosphate standard. Specific activity was determined as the amount of picomoles of phosphate released per minute per microgram of protein.

Laser scanning confocal microscopy analysis

HEK cells (1×10^5) were seeded and grown overnight on coverslips and fixed in 4% formaldehyde for 15 min and permeabilized in 0.2% Triton X-100. The cells were then incubated in blocking solution (3% FBS in PBS) for 30 min at 37°C and followed by incubation with specific antibodies overnight. Alexa Fluor 488 and Alexa Fluor 594-conjugated IgG second antibody (1:1000) was incubated for 1 h. The slides were counter-stained with 4',6-Diamidino-2-phenylindole (DAPI, 1 μg/ml) and observed under a LSM510 META laser scanning confocal microscope (Leica TCS SP5) with ×200 magnification..

Neutral Comet assay

Cells were treated with CPT (2 μM) or DMSO for 1 h and recovered for indicated time points. Cells at a density of 5×10^4 cells/ml were mixed gently with

pre-melted low-temperature-melting agarose at a volume ratio of 1 to 10 (v/v) and spread on glass slides. Slides were subsequently placed in a pre-cooled lysis buffer (2 M NaCl, 30 mM Na_2EDTA, 10 mM Tris-HCl, 1% Triton X-100, and 10% DMSO, pH 8.0) at 4°C for 1 h. After lysis, the slides were equilibrated in an alkaline rinse solution (0.3 M NaOH, 1mM EDTA), electrophoresed at 0.7 V/cm for 20 min and stained with PI. Comet images were examined at 200× magnifications using a fluorescence microscope (Nikon, ECLIPSE Ti) and digitized. The tail moment values (TM) were quantified under microscope and analyzed by Comet Score software (Freeware v1.5).

Cytokinesis-block micronucleus assay (CBMN)

Duplicate cultures of HEK cells were treated with 0.08 μg/ml MMC for 24 h, then cytokinesis was blocked with 6 μg/ml of cytochalasin B (cyt-B) for 36 h before harvest. After hypotonic treatment, the cells were fixed with 3:1 methanol/glacial acetic acid, dropped onto a clean microscopic slide, air-dried and stained with 3% Giemsa solution in 0.075 M PBS (pH 6.8). All slides were chilled and scored blindly by an experienced scorer. A total of 1000 binucleated (BN) cells for each subject were examined microscopically for micronuclei (MN) according to the scoring criteria outlined by HUMN Project (Kanaar and Hoeijmakers, 1998).

Non-homologous end joining (NHEJ) and homologous recombination (HR) DNA repair assays

For NHEJ, HEK 293T cells were transfected with vectors encoding respective shRNAs against GFP and α4 or B56ε, then selected with puromycin for 24 h. Following puromycin selection, cells were co-transfected with pBabe-GFP linearized by Hind III together with pBabe-HcRed plasmid. The efficiency of NHEJ was assessed by the number of GFP/HcRed-positive cells 48 h after transfection by flow

cytometry analysis using a FACSCanto (BD biosciences).

HR DNA repair efficiency was analyzed using 293 DR-GFP cells, which contain a stably integrated copy of the transgenic reporter DR-GFP (Weinstock et al., 2006). 293 DR-GFP cells were transfected with specific shRNAs targeting luciferase, α4, and B56ε. After puromycin selection, the cells were transfected with I-SceI expression vector. The number of GFP-positive cells was measured 48 h later by flow cytometry analysis using a FACSCanto.

Statistical analysis

Data are presented as mean ± SD from three independent experiments. All data were analyzed using SPSS 13.0. Unless indicated, the differences between two groups were analyzed using Student's t-test. The comparisons of frequencies of micronuclei between groups were performed by one-way ANOVA first and followed by Dunnett's t-test. Differences were considered statistically significant at $P<0.05$.

Acknowledgements

This work was supported by the National Key Basic Research and Development Program (2010CB912803 to W.C.), the National Nature Science Foundation of China (NSFC) (30925029 to W.C., 81072284 to Y.-M.X., 30901211 to B.Z., and 81102158 to Y.-D.L.), the Guangdong Province Universities and Colleges Pearl River Scholar Funded Scheme (GDUPS 2010 to W.C.), the FWO (ZKC2592-00_WO1 to A.S.), and the National Institutes of Health/National Cancer Institute (P01 CA0506 to W.-C.H.).

Author contributions

LPC conducted experiments and wrote the manuscript. YDL and XNZ conducted the Comet assay and CBMN experiments. LM and QB generated cells lines expressing shRNAs targeting each PP2A subunits and measured the phosphatase activity. IV and ZBZ conducted NHEJ and HR DNA repair assays. AAS and WCH contributed to experimental design and manuscript revision. WC was responsible for experimental design, financially supported the experiments and revised the manuscript.

References

Abbotts, R., Thompson, N. and Madhusudan, S. (2014). DNA repair in cancer: emerging targets for personalized therapy. *Cancer Manag Res* **6**, 77-92.

Barsoum, J. and Varshavsky, A. (1985). Preferential localization of variant nucleosomes near the 5'-end of the mouse dihydrofolate reductase gene. *Journal of Biological Chemistry* **260**, 7688-97.

Bartek, J. and Lukas, J. (2007). DNA damage checkpoints: from initiation to recovery or adaptation. *Curr Opin Cell Biol* **19**, 238-45.

Celeste, A., Difilippantonio, S., Difilippantonio, M. J., Fernandez-Capetillo, O., Pilch, D. R., Sedelnikova, O. A., Eckhaus, M., Ried, T., Bonner, W. M. and Nussenzweig, A. (2003). H2AX haploinsufficiency modifies genomic stability and tumor susceptibility. *Cell* **114**, 371-83.

Celeste, A., Petersen, S., Romanienko, P. J., Fernandez-Capetillo, O., Chen, H. T., Sedelnikova, O. A., Reina-San-Martin, B., Coppola, V., Meffre, E., Difilippantonio, M. J. et al. (2002). Genomic instability in mice lacking histone H2AX. *Science* **296**, 922-7.

Cha, H., Lowe, J. M., Li, H., Lee, J. S., Belova, G. I., Bulavin, D. V. and Fornace, A. J., Jr. (2010). Wip1 directly dephosphorylates gamma-H2AX and attenuates the DNA damage response. *Cancer Res* **70**, 4112-22.

Chen, L. P., Lai, Y. D., Li, D. C., Zhu, X. N., Yang, P., Li, W. X., Zhu, W., Zhao, J., Li, X. D., Xiao, Y. M. et al. (2011). alpha4 is highly expressed in carcinogen-transformed human cells and primary human cancers. *Oncogene* **30**, 2943-53.

Chen, W., Arroyo, J. D., Timmons, J. C., Possemato, R. and Hahn, W. C. (2005). Cancer-associated PP2A Aalpha subunits induce functional haploinsufficiency and tumorigenicity. *Cancer Res* **65**, 8183-92.

Chen, W., Possemato, R., Campbell, K. T., Plattner, C. A., Pallas, D. C. and Hahn, W. C. (2004). Identification of specific PP2A complexes involved in human cell transformation. *Cancer Cell* **5**, 127-36.

Chowdhury, D., Keogh, M. C., Ishii, H., Peterson, C. L., Buratowski, S. and Lieberman, J. (2005). gamma-H2AX dephosphorylation by protein phosphatase 2A facilitates DNA double-strand break repair. *Mol Cell* **20**, 801-9.

Chowdhury, D., Xu, X., Zhong, X., Ahmed, F., Zhong, J., Liao, J., Dykxhoorn, D. M., Weinstock, D. M., Pfeifer, G. P. and Lieberman, J. (2008). A PP4-phosphatase complex dephosphorylates gamma-H2AX generated during DNA replication. *Mol Cell* **31**, 33-46.

Di Como, C. J. and Arndt, K. T. (1996). Nutrients, via the Tor proteins, stimulate the

association of Tap42 with type 2A phosphatases. *Genes & Development* **10**, 1904-16.

Douglas, P., Zhong, J., Ye, R., Moorhead, G. B., Xu, X. and Lees-Miller, S. P. (2010). Protein phosphatase 6 interacts with the DNA-dependent protein kinase catalytic subunit and dephosphorylates gamma-H2AX. *Mol Cell Biol* **30**, 1368-81.

Fenech, M. (2002). Chromosomal biomarkers of genomic instability relevant to cancer. *Drug Discovery Today* **7**, 1128-37.

Fernandez-Capetillo, O., Chen, H. T., Celeste, A., Ward, I., Romanienko, P. J., Morales, J. C., Naka, K., Xia, Z., Camerini-Otero, R. D., Motoyama, N. et al. (2002). DNA damage-induced G2-M checkpoint activation by histone H2AX and 53BP1. *Nature Cell Biology* **4**, 993-7.

Fernandez-Capetillo, O., Lee, A., Nussenzweig, M. and Nussenzweig, A. (2004). H2AX: the histone guardian of the genome. *DNA Repair (Amst)* **3**, 959-67.

Fillingham, J., Keogh, M. C. and Krogan, N. J. (2006). GammaH2AX and its role in DNA double-strand break repair. *Biochemistry and Cell Biology* **84**, 568-77.

Grochola, L. F., Vazquez, A., Bond, E. E., Wurl, P., Taubert, H., Muller, T. H., Levine, A. J. and Bond, G. L. (2009). Recent natural selection identifies a genetic variant in a regulatory subunit of protein phosphatase 2A that associates with altered cancer risk and survival. *Clinical Cancer Research* **15**, 6301-8.

Guzi, T. J., Paruch, K., Dwyer, M. P., Labroli, M., Shanahan, F., Davis, N., Taricani, L., Wiswell, D., Seghezzi, W., Penaflor, E. et al. (2011). Targeting the replication checkpoint using SCH 900776, a potent and functionally selective CHK1 inhibitor identified via high content screening. *Molecular Cancer Therapeutics* **10**, 591-602.

Hahn, W. C., Counter, C. M., Lundberg, A. S., Beijersbergen, R. L., Brooks, M. W. and Weinberg, R. A. (1999). Creation of human tumour cells with defined genetic elements. *Nature* **400**, 464-8.

Harding, S. M., Coackley, C. and Bristow, R. G. (2011). ATM-dependent phosphorylation of 53BP1 in response to genomic stress in oxic and hypoxic cells. *Radiother Oncol* **99**, 307-12.

Huertas, P. (2010). DNA resection in eukaryotes: deciding how to fix the break. *Nature Structural & Molecular Biology* **17**, 11-6.

Jackson, S. P. (2002). Sensing and repairing DNA double-strand breaks. *Carcinogenesis* **23**, 687-96.

Janssens, V. and Goris, J. (2001). Protein phosphatase 2A: a highly regulated family of serine/threonine phosphatases implicated in cell growth and signalling. *Biochemical Journal* **353**,

417-39.

Jin, Z., Wallace, L., Harper, S. Q. and Yang, J. (2010). PP2A:B56{epsilon}, a substrate of caspase-3, regulates p53-dependent and p53-independent apoptosis during development. *Journal of Biological Chemistry* **285**, 34493-502.

Kalev, P., Simicek, M., Vazquez, I., Munck, S., Chen, L., Soin, T., Danda, N., Chen, W. and Sablina, A. (2012a). Loss of PPP2R2A inhibits homologous recombination DNA repair and predicts tumor sensitivity to PARP inhibition. *Cancer Research*.

Kalev, P., Simicek, M., Vazquez, I., Munck, S., Chen, L., Soin, T., Danda, N., Chen, W. and Sablina, A. (2012b). Loss of PPP2R2A inhibits homologous recombination DNA repair and predicts tumor sensitivity to PARP inhibition. *Cancer Research* **72**, 6414-24.

Kanaar, R. and Hoeijmakers, J. H. (1998). Genetic recombination. From competition to collaboration. *Nature* **391**, 335, 337-8.

Keogh, M. C., Kim, J. A., Downey, M., Fillingham, J., Chowdhury, D., Harrison, J. C., Onishi, M., Datta, N., Galicia, S., Emili, A. et al. (2006). A phosphatase complex that dephosphorylates gammaH2AX regulates DNA damage checkpoint recovery. *Nature* **439**, 497-501.

Kinner, A., Wu, W., Staudt, C. and Iliakis, G. (2008). Gamma-H2AX in recognition and signaling of DNA double-strand breaks in the context of chromatin. *Nucleic Acids Research* **36**, 5678-94.

Kloeker, S., Reed, R., McConnell, J. L., Chang, D., Tran, K., Westphal, R. S., Law, B. K., Colbran, R. J., Kamoun, M., Campbell, K. S. et al. (2003). Parallel purification of three catalytic subunits of the protein serine/threonine phosphatase 2A family (PP2A(C), PP4(C), and PP6(C)) and analysis of the interaction of PP2A(C) with alpha4 protein. *Protein Expression and Purification* **31**, 19-33.

Kolas, N. K., Chapman, J. R., Nakada, S., Ylanko, J., Chahwan, R., Sweeney, F. D., Panier, S., Mendez, M., Wildenhain, J., Thomson, T. M. et al. (2007). Orchestration of the DNA-damage response by the RNF8 ubiquitin ligase. *Science* **318**, 1637-40.

Kong, M., Ditsworth, D., Lindsten, T. and Thompson, C. B. (2009). Alpha4 is an essential regulator of PP2A phosphatase activity. *Molecular Cell* **36**, 51-60.

Kong, M., Fox, C. J., Mu, J., Solt, L., Xu, A., Cinalli, R. M., Birnbaum, M. J., Lindsten, T. and Thompson, C. B. (2004). The PP2A-associated protein alpha4 is an essential inhibitor of apoptosis. *Science* **306**, 695-8.

Kusch, T., Florens, L., Macdonald, W. H., Swanson, S. K., Glaser, R. L., Yates, J. R., 3rd,

Abmayr, S. M., Washburn, M. P. and Workman, J. L. (2004). Acetylation by Tip60 is required for selective histone variant exchange at DNA lesions. *Science* **306**, 2084-7.

McConnell, J. L., Watkins, G. R., Soss, S. E., Franz, H. S., McCorvey, L. R., Spiller, B. W., Chazin, W. J. and Wadzinski, B. E. (2010). Alpha4 is a ubiquitin-binding protein that regulates protein serine/threonine phosphatase 2A ubiquitination. *Biochemistry* **49**, 1713-8.

McCright, B., Rivers, A. M., Audlin, S. and Virshup, D. M. (1996). The B56 family of protein phosphatase 2A (PP2A) regulatory subunits encodes differentiation-induced phosphoproteins that target PP2A to both nucleus and cytoplasm. *Journal of Biological Chemistry* **271**, 22081-9.

Melander, F., Bekker-Jensen, S., Falck, J., Bartek, J., Mailand, N. and Lukas, J. (2008). Phosphorylation of SDT repeats in the MDC1 N terminus triggers retention of NBS1 at the DNA damage-modified chromatin. *Journal of Cell Biology* **181**, 213-26.

Moffat, J., Grueneberg, D. A., Yang, X., Kim, S. Y., Kloepfer, A. M., Hinkle, G., Piqani, B., Eisenhaure, T. M., Luo, B., Grenier, J. K. et al. (2006). A lentiviral RNAi library for human and mouse genes applied to an arrayed viral high-content screen. *Cell* **124**, 1283-98.

Murnane, J. P. (2010). Telomere loss as a mechanism for chromosome instability in human cancer. *Cancer Res* **70**, 4255-9.

Nabb, M. T., Kimber, L., Haines, A. and McCourt, C. (2006). Does regular massage from late pregnancy to birth decrease maternal pain perception during labour and birth?--A feasibility study to investigate a programme of massage, controlled breathing and visualization, from 36 weeks of pregnancy until birth. *Complement Ther Clin Pract* **12**, 222-31.

Nakada, S., Chen, G. I., Gingras, A. C. and Durocher, D. (2008). PP4 is a gamma H2AX phosphatase required for recovery from the DNA damage checkpoint. *EMBO Rep* **9**, 1019-26.

Nanahoshi, M., Tsujishita, Y., Tokunaga, C., Inui, S., Sakaguchi, N., Hara, K. and Yonezawa, K. (1999). Alpha4 protein as a common regulator of type 2A-related serine/threonine protein phosphatases. *FEBS Letters* **446**, 108-12.

Prickett, T. D. and Brautigan, D. L. (2004). Overlapping binding sites in protein phosphatase 2A for association with regulatory A and alpha-4 (mTap42) subunits. *Journal of Biological Chemistry* **279**, 38912-20.

Reid, M. A., Wang, W. I., Rosales, K. R., Welliver, M. X., Pan, M. and Kong, M. (2013). The B55alpha Subunit of PP2A Drives a p53-Dependent Metabolic Adaptation to Glutamine Deprivation. *Molecular Cell*.

Rogakou, E. P., Boon, C., Redon, C. and Bonner, W. M. (1999). Megabase chromatin

domains involved in DNA double-strand breaks in vivo. *Journal of Cell Biology* **146**, 905-16.

Rogakou, E. P., Pilch, D. R., Orr, A. H., Ivanova, V. S. and Bonner, W. M. (1998). DNA double-stranded breaks induce histone H2AX phosphorylation on serine 139. *Journal of Biological Chemistry* **273**, 5858-68.

Rothkamm, K. and Lobrich, M. (2003). Evidence for a lack of DNA double-strand break repair in human cells exposed to very low x-ray doses. *Proceedings of the National Academy of Sciences of the United States of America* **100**, 5057-62.

Sents, W., Ivanova, E., Lambrecht, C., Haesen, D. and Janssens, V. (2013). The biogenesis of active protein phosphatase 2A holoenzymes: a tightly regulated process creating phosphatase specificity. *FEBS Journal* **280**, 644-61.

Shao, R. G., Cao, C. X., Zhang, H., Kohn, K. W., Wold, M. S. and Pommier, Y. (1999). Replication-mediated DNA damage by camptothecin induces phosphorylation of RPA by DNA-dependent protein kinase and dissociates RPA:DNA-PK complexes. *EMBO J* **18**, 1397-406.

Shi, Y. (2009). Serine/threonine phosphatases: mechanism through structure. *Cell* **139**, 468-84.

Shouse, G. P., Nobumori, Y., Panowicz, M. J. and Liu, X. (2011). ATM-mediated phosphorylation activates the tumor-suppressive function of B56gamma-PP2A. *Oncogene* **30**, 3755-65.

Shrivastav, M., De Haro, L. P. and Nickoloff, J. A. (2008). Regulation of DNA double-strand break repair pathway choice. *Cell Research* **18**, 134-47.

Smetana, J. H., Oliveira, C. L., Jablonka, W., Aguiar Pertinhez, T., Carneiro, F. R., Montero-Lomeli, M., Torriani, I. and Zanchin, N. I. (2006). Low resolution structure of the human alpha4 protein (IgBP1) and studies on the stability of alpha4 and of its yeast ortholog Tap42. *Biochimica et Biophysica Acta* **1764**, 724-34.

Sonoda, E., Hochegger, H., Saberi, A., Taniguchi, Y. and Takeda, S. (2006). Differential usage of non-homologous end-joining and homologous recombination in double strand break repair. *DNA Repair (Amst)* **5**, 1021-9.

Strack, S., Zaucha, J. A., Ebner, F. F., Colbran, R. J. and Wadzinski, B. E. (1998). Brain protein phosphatase 2A: developmental regulation and distinct cellular and subcellular localization by B subunits. *Journal of Comparative Neurology* **392**, 515-27.

Strumberg, D., Pilon, A. A., Smith, M., Hickey, R., Malkas, L. and Pommier, Y. (2000). Conversion of topoisomerase I cleavage complexes on the leading strand of ribosomal DNA into 5'-phosphorylated DNA double-strand breaks by replication runoff. *Mol Cell Biol* **20**, 3977-87.

Stucki, M., Clapperton, J. A., Mohammad, D., Yaffe, M. B., Smerdon, S. J. and Jackson, S. P. (2005). MDC1 directly binds phosphorylated histone H2AX to regulate cellular responses to DNA double-strand breaks. *Cell* **123**, 1213-26.

Stucki, M. and Jackson, S. P. (2006). gammaH2AX and MDC1: anchoring the DNA-damage-response machinery to broken chromosomes. *DNA Repair (Amst)* **5**, 534-43.

Tomita, M. (2010). Involvement of DNA-PK and ATM in radiation- and heat-induced DNA damage recognition and apoptotic cell death. *Journal of Radiation Research* **51**, 493-501.

Trockenbacher, A., Suckow, V., Foerster, J., Winter, J., Krauss, S., Ropers, H. H., Schneider, R. and Schweiger, S. (2001). MID1, mutated in Opitz syndrome, encodes an ubiquitin ligase that targets phosphatase 2A for degradation. *Nature Genetics* **29**, 287-94.

Valdiglesias, V., Giunta, S., Fenech, M., Neri, M. and Bonassi, S. (2013). gammaH2AX as a marker of DNA double strand breaks and genomic instability in human population studies. *Mutation Research*.

Weinstock, D. M., Nakanishi, K., Helgadottir, H. R. and Jasin, M. (2006). Assaying double-strand break repair pathway choice in mammalian cells using a targeted endonuclease or the RAG recombinase. *Methods in Enzymology* **409**, 524-40.

Xu, Y. and Price, B. D. (2011). Chromatin dynamics and the repair of DNA double strand breaks. *Cell Cycle* **10**, 261-7.

Xu, Y., Xing, Y., Chen, Y., Chao, Y., Lin, Z., Fan, E., Yu, J. W., Strack, S., Jeffrey, P. D. and Shi, Y. (2006). Structure of the protein phosphatase 2A holoenzyme. *Cell* **127**, 1239-51.

Yang, J., Roe, S. M., Prickett, T. D., Brautigan, D. L. and Barford, D. (2007). The structure of Tap42/alpha4 reveals a tetratricopeptide repeat-like fold and provides insights into PP2A regulation. *Biochemistry* **46**, 8807-15.

Zhao, Y., Boguslawski, G., Zitomer, R. S. and DePaoli-Roach, A. A. (1997). Saccharomyces cerevisiae homologs of mammalian B and B' subunits of protein phosphatase 2A direct the enzyme to distinct cellular functions. *Journal of Biological Chemistry* **272**, 8256-62.

Figure legends

Fig 1. Suppression of specific PP2A regulatory subunits leads to persistence of γ-H2AX. (A) Immunoblotting analysis of γ-H2AX at 12 h after vehicle (DMSO) (C) or 2 μM CPT treatment (T) in HEK cells expressing shRNAs against each of PP2A subunits. Suppression of PP2A B subunits was confirmed by immunoblotting with the indicated antibodies. (B) γ-H2AX levels in HEK expressing the indicated shRNAs treated with 2 μM CPT for 1 h. Immunoblotting analysis of γ-H2AX was performed at different time points after removal of CPT. (C) Immunofluorescence (IF) analysis of γ-H2AX was performed at different time points after CPT treatment in HEK SHGFP, SHB55α, SHB56γ, SHB56ε, and SHα4 cells. Data are shown as the mean number of γ-H2AX foci per nucleus ± SEM for three independent experiments. $P<0.05$ (*) compared to HEK SHGFP cells, as determined by the Student *t*-test.

Fig 2. PP2A B56ε holoenzyme is responsible for γ-H2AX dephosphorylation. (A) B56ε and α4 interact with γ-H2AX. 48 h post-transfection with HA-tagged B55α, B56γ, B56ε, or α4 293FT cells were treated with 2 μM CPT for 1 h and allowed to recover for 5 h. HA-tagged proteins were co-immunoprecipitated (co-IP) with anti-HA-agarose followed by immunoblotting using anti-γ-H2AX or anti-PP2Ac antibody. VT refers to empty vector. (B) γ-H2AX forms complexes with different PP2A subunits. Soluble nuclear fraction was isolated from CPT-treated 293FT cells 5 h after recovery. Co-IP was performed using the indicated antibodies. (C) Wild type H2AX (WT-H2AX) but not Ser139Ala H2AX mutant (Mut-H2AX) interacts with PP2A specific subunits. 48 h post-transfection with HA-tagged H2AX 293FT cells were treated with 2 μM CPT for 1 h and allowed to recover for 5 h. Nuclear fractions were isolated from CPT-treated cells and HA-tagged H2AX was co-IP with anti-HA antibody followed by immunoblotting with the indicated antibodies. (D) B56ε co-localizes with γ-H2AX upon DNA damage. HEK cells expressing HA-tagged B55α, B56γ, and B56ε were treated with CPT and recovered for the indicated periods

of time. Immunofluorescence analysis was performed using antibodies against HA-tag (*green*) and γ-H2AX (*red*). The merge ratio of two proteins, B56ε and γ-H2AX in 50 cells was calculated. (E) Cellular distribution of PP2A subunits upon DNA damage. 293FT cells were treated with CPT and allowed to recover at 1 h (T1), 5 h (T5), and 10 h (T10). Expression of the indicated proteins in cytoplasmic and nuclear fractions of the CPT-treated cells was detected by immunoblotting. GAPDH and lamin B1 were used as the loading controls for cytoplasmic and nuclear fractions, respectively.

Fig 3. α4 is essential for recruitment of PP2A B56ε holoenzyme to γ-H2AX foci. (A) γ-H2AX binds distinct PP2A complexes during DNA repair process. 293FT cells were treated with CPT and allowed to recover for 1 h, 5 h or 10 h. The nuclear fractions of CPT-treated cells were subjected to co-IP with antibodies against PP2Ac or γ-H2AX. (B) PP2A activity in nuclear fraction during DNA repair. PP2A-attributable activity was detected using mononucleosomes as a substrate in control cells (C) and cells with recovery for the indicated time points after CPT treatment. *, $P<0.05$ compared to the control. Immunoblotting analysis of PP2Ac and γ-H2AX in mononucleosome isolated from 293FT cells treated with CPT for 1 h. (C) α4 depletion does not affect subcellular localization of B56ε. HEK SHGFP and SHα4 cells were treated with CPT (T) or vehicle (DMSO) (C) and allowed to recover for 5 h. Immunoblotting analysis of the indicated proteins was performed using cytoplasmic (C) and nuclear fractions (N). (D) Suppression of α4 affects γ-H2AX/B56ε complexes formation. 48 h after transfection with shGFP or shα4 239FT cells were treated with CPT and recovered for 5 h. Nuclear fractions isolated from CPT-treated cells were co-IP with antibodies against γ-H2AX or PP2Ac followed by immunoblotting analysis with the indicated antibodies.

Fig 4. Loss of PP2A B56ε or α4 impairs DNA repair and increases cell sensitivity to DNA damage. (A) The degree of DNA damage in CPT-treated cells after

suppression of specific PP2A subunits was determined by the single-cell gel electrophoresis (Comet assay). Images were taken under fluorescence microscope with 100×magnification. The representative images are shown for HEK SHGFP, SHB56γ, SHB56ε, or SHα4 cells 2 h or 12 h following 2 μM CPT treatments. The relative comet tail moments (TM) of 75 cells normalized to control cells (C) are present as mean ± SEM. $P<0.05$ (*) compared to SHGFP, as determined by Student *t*-test. (B) Micronucleus test in HEK SHGFP, SHB56γ, SHB56ε, or SHα4 cells treated with MMC (0.08 μg/ml) or DMSO for 24 h. The frequency of micronuclei (MN) in 1000 binucleated (BN) cells is presented as mean ± SEM for three independent experiments. *$P<0.05$ compared to the SHGFP control, as determined by One-way ANOVA first and followed by Dunnett's *t*-test. (C) The efficiency of I-SceI–induced NHEJ repair in H1299dA3-1 cells expressing shRNAs specific to GFP, B56γ, B56ε, or α4. (D) The efficiency of I-SceI–induced HR repair in 293 DR-GFP cells expressing the indicated shRNAs specific to GFP, B56γ, B56ε, or α4. $P<0.05$ (*) compared to SHGFP, as determined by Student *t*-test.

Fig 5. Overexpression of PP2A B56ε and α4 cooperates to promote the DNA repair. (A) Immunoblotting analysis of B56ε and α4 in HEK cells expressing individual B56ε, or α4, or co-expressing both B56ε and α4 (B56ε-α4). (B) Dynamic changes of γ-H2AX levels in HEK cells expressing the indicated genes and treated with 2 μM CPT for 1 h. (C) The Comet assay was performed in these HEK cells. The relative comet tail moments (TM) of 75 cells normalized to control cells are present as mean ± SEM. $P<0.05$ (*) compared to vector, as determined by Student *t*-test. (D) The efficiency of I-SceI–induced NHEJ repair in H1299dA3-1 cells expressing indicated genes. (E) The efficiency of I-SceI–induced HR repair in 293 DR-GFP cells expressing the indicated genes. $P<0.05$ (*) compared to Vector, as determined by Student *t*-test.

Fig 6. Expression of PP2A B56ε or α4 is up-regulated in carcinogen-transformed hepatocytes and primary human cancers. (A) Immunoblotting analysis of B56ε or α4 in non-malignant L02 cells, AFB_1-transformed cells (L02RT-AFB_1). Fold change of B56ε or α4 levels normalized to β-actin expression are indicated. (B) Dynamic changes of γ-H2AX in hepatocytes treated with 2 μM of CPT for 1 h and recovered for different time points. Fold change of γ-H2AX level normalized to β-actin are indicated. (C) Comet assay of L02, transformed L02RT-AFB_1 cells at 2 h or 12 h following 2 μM CPT treatments removal. The relative comet tail moments (TM) of 75 cells normalized to control cells (C) are present as mean ± SEM. $P<0.05$ (*) compared to L02 cells as determined by Student *t*-test. (D) Immunoblotting analysis of B56ε, α4, or γ-H2AX expression in 14 pairs of HCC samples with matched adjacent non-tumor tissues. Up-regulation of B56ε, α4, or γ-H2AX levels (T/N) was calculated as the fold of these proteins in tumor tissues to the adjacent non-tumor tissues using densitometry analysis after normalization to β-actin. (E) The cell cycle analysis was performed in cells indicated. The percentage of the G1, S, and G2/M phase in the cell cycle at 8 h after CPT treatment in HEK cells expressing individual B56ε, or α4, or both B56ε-α4. The percentages of each phase of the cell cycle were analyzed using ModFit software.

Figure 1

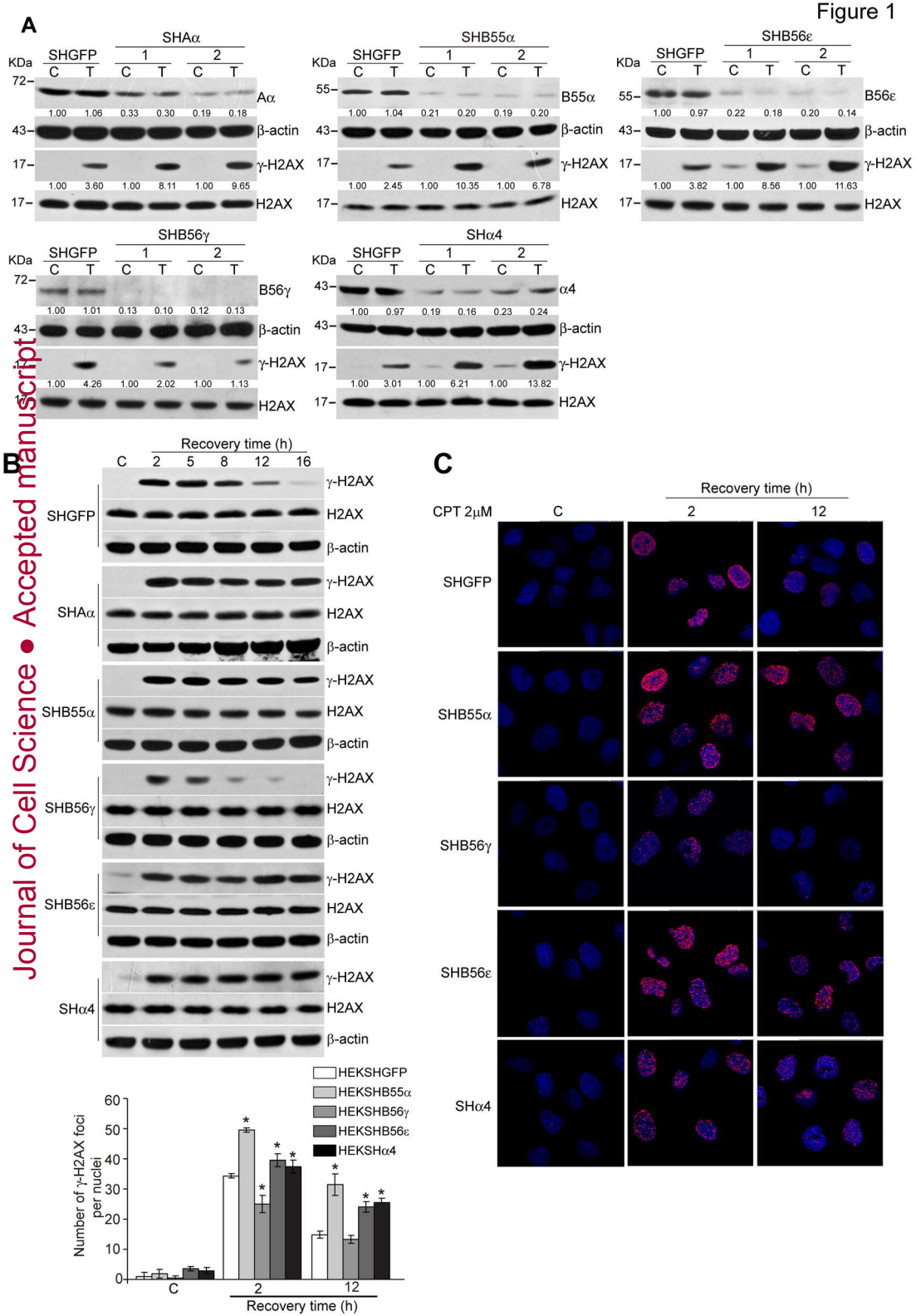

Figure 2